Virology 390 (2009) 268–278

Contents lists available at ScienceDirect

Virology

journal homepage: www.elsevier.com/locate/yviro

Budding of filamentous and non-filamentous influenza A virus occurs via a VPS4 and VPS28-independent pathway

Emily A. Bruce [a], Liz Medcalf [a,1], Colin M. Crump [a], Sarah L. Noton [a,2], Amanda D. Stuart [a], Helen M. Wise [a], Debra Elton [a,1], Katherine Bowers [b], Paul Digard [a,*]

[a] Division of Virology, Department of Pathology, University of Cambridge, Tennis Court Road, Cambridge CB2 1QP, UK
[b] Institute of Structural and Molecular Biology, Division of Biosciences, University College London, WC1E 6BT, UK

ARTICLE INFO

Article history:
Received 11 March 2009
Returned to author for revision 2 April 2009
Accepted 8 May 2009
Available online 13 June 2009

Keywords:
Assembly
ESCRT
VPS28-1
VPS28-2
Multivesicular body

ABSTRACT

The mechanism of membrane scission during influenza A virus budding has been the subject of controversy. We confirm that influenza M1 binds VPS28, a subunit of the ESCRT-1 complex. However, confocal microscopy of infected cells showed no marked colocalisation between M1 and VPS28 or VPS4 ESCRT proteins, or relocalisation of the cellular proteins. Trafficking of HA and M1 appeared normal when endosomal sorting was impaired by expression of inactive VPS4. Overexpression of either isoform of VPS28 or wildtype or dominant negative VPS4 proteins did not alter production of filamentous virions. SiRNA depletion of endogenous VPS28 had no significant effect on influenza virus replication. Furthermore, cells expressing wildtype or dominant-negative VPS4 replicated filamentous and non-filamentous strains of influenza to similar titres, indicating that influenza release is VPS4-independent. Overall, we see no role for the ESCRT pathway in influenza virus budding and the significance of the M1–VPS28 interaction remains to be determined.

Introduction

A member of the *Orthomyxoviridae* family, influenza A virus can form two morphologically distinct types of enveloped particles; spherical and filamentous virions (Mosley and Wyckoff, 1946). Filamentous influenza particles have the same diameter as spherical ones (approximately 100 nm) but can reach over 30 μm in length (Roberts and Compans, 1998). Both types of virion contain the same set of viral proteins: the haemagglutinin (HA) and neuraminidase (NA) glycoproteins, and M2 ion channel embedded in the host-derived lipid bilayer, surrounding an internal layer of the M1 matrix protein which in turn encapsidates the genomic ribonucleoproteins (RNPs) along with small quantities of the NS2/NEP protein (Cheung and Poon, 2007). Individual strains of influenza virus vary in whether they produce only spherical or a mixture of spherical and filamentous particles, with the loss of filamentous virus formation being associated with adaptation to growth in eggs (Choppin and Tamm, 1960; Kilbourne and Murphy, 1960). Virion morphology is determined by a combination of viral genetics and cellular factors. M1 is the major determinant of particle shape (Bourmakina and Garcia-Sastre, 2003; Elleman and Barclay, 2004) although other virus genes also play a role (Jin et al., 1997; Mitnaul et al., 1996; Roberts et al., 1998; Smirnov Yu et al., 1991). In the laboratory, polarised epithelial cells produce more filamentous virus than non-polarised cells, potentially due to the organisation of the actin cytoskeleton (Roberts and Compans, 1998; Simpson-Holley et al., 2002). However, cells with an intermediate epithelioid phenotype such as 293T cells, that do not possess fully differentiated apical and basolateral plasma membrane surfaces but grow in adherent sheets are able to support filament production (data not shown).

Whether the mature virion is filamentous or spherical, its final release requires 'pinching off' of the viral envelope from the plasma membrane. While it seems probable that cellular proteins are involved in this final membrane scission step, this issue has not yet been resolved. The matrix proteins of many other enveloped viruses contain 'late domains'; short interchangeable peptide motifs that interact with and co-opt the cellular Endosomal Sorting Complex Required for Transport (ESCRT) system in order to bud outwards from the plasma membrane (reviewed in Morita and Sundquist, 2004). The ESCRT pathway comprises four multi-protein complexes (termed ESCRT-0 to ESCRT-III) that are normally involved in membrane remodelling processes such as multivesicular body (MVB) biogenesis and cytokinesis (Stuffers et al., 2008). ESCRT proteins were originally identified in yeast in screens for genes affecting protein trafficking to the vacuole (vacuole protein sorting, *VPS* genes) (Bankaitis et al.,

* Corresponding author. Fax: +44 1223 336926.
E-mail address: pd1@mole.bio.cam.ac.uk (P. Digard).
[1] Present address: Animal Health Trust, Lanwades Park, Kentford, Newmarket, Suffolk CB8 7UU, UK.
[2] Present address: Department of Microbiology, Boston University School of Medicine, Boston, Massachusetts, 02118, USA.

0042-6822/$ – see front matter © 2009 Elsevier Inc. All rights reserved.
doi:10.1016/j.virol.2009.05.016

1986; Rothman and Stevens, 1986). Mutation of the class E group of *VPS* genes results in a phenotype whereby proteins accumulate in a large, aberrant endosomal compartment adjacent to the vacuole (Raymond et al., 1992). Later work established that the ESCRT machinery is highly conserved from yeast to man (Katzmann et al., 2001). ESCRTs play an important role in trafficking ubiquitinated proteins from endosomes to lysosomes for degradation, by recognising the ubiquitin signal and targeting the protein for inclusion into the inward-budding vesicles of the MVB. ESCRTs are also proposed to function in the inward-budding process itself. As noted above, this structural feature has been hijacked by several viruses for their final membrane scission step, either into an internal lumen, or from the plasma membrane (Chen and Lamb, 2008). Viruses known to use the ESCRT pathway include many retroviruses such as human immunodeficiency virus (HIV) (Garrus et al., 2001; Martin-Serrano et al., 2001) and murine leukemia virus (MLV) (Garrus et al., 2001), as well as viruses from other families such as vesicular stomatitis virus (Taylor et al., 2007) and herpes simplex virus (HSV) (Crump et al., 2007). Disruption of ESCRT function or mutation of viral late domains generally prevents the separation of virions from the cell membrane, often resulting in 'daisy-chain' or sometimes in filamentous particle morphologies (Bieniasz, 2006). The striking similarities in virion morphology of some HIV and MLV late domain mutants (Bieniasz, 2006; Yuan et al., 2000) and filamentous influenza virus particles (Roberts and Compans, 1998; Simpson-Holley et al., 2002) prompted us to hypothesise that influenza virus also used the ESCRT system to bud, and that formation of filamentous viral particles was the result of a reduced ability to engage ESCRT complexes. In initial support of this, two studies suggested that influenza A M1 contained a 'late domain' that interacted with the ESCRT protein VPS28 to direct virus budding (Hui et al., 2003, 2006a), while a further report from another laboratory showed that a point mutation in the putative late domain promoted the formation of filamentous particles (Burleigh et al., 2005). However, much of the evidence supporting the use of the ESCRT pathway by influenza rested on the behaviour of sets of supposedly viable recombinant viruses which showed that, similarly to other virus families, the influenza M1 late domain was replaceable by alternative late domain sequences and could be moved elsewhere in the protein. Unfortunately, the realisation that these viruses were in fact WT influenza and the subsequent retraction of the papers by Hui et al. (2006b) left the role of the ESCRT pathway in influenza virus budding uncertain. Indeed, a later study examining the requirements for budding of recombinant influenza A virus like particles (VLPs) found that their production did not require a functional ESCRT pathway (Chen et al., 2007).

Here, we further examine the interaction of influenza A virus with the ESCRT pathway. We show that although the M1 protein binds VPS28 protein *in vitro*, budding of both filamentous and non-filamentous strains of virus is independent of VPS28 levels and a functional VPS4 in epithelial and epithelioid cell lines.

Results

Interactions between the influenza A M1 protein and VPS28

Prompted by the publication (but prior to its retraction) of the study by Hui et al. (2006a, 2006b) suggesting a functionally important interaction between VPS28 and influenza A M1 involved in virus budding, we set out to test the hypothesis that the strength of the interaction between M1 and VPS28 controls virus particle morphology by determining the efficiency with which nascent virions pinch off from the plasma membrane. To this end, VPS28-1 and VPS28-2 isoforms were expressed and purified from *Escherichia coli* as glutathione-*S*-transferase (GST) fusion proteins, as well as similar fusion proteins containing the influenza A/PR/8/34 (PR8) M1 and NP proteins (Fig. 1a, panel i). When the VPS28 constructs were tested for

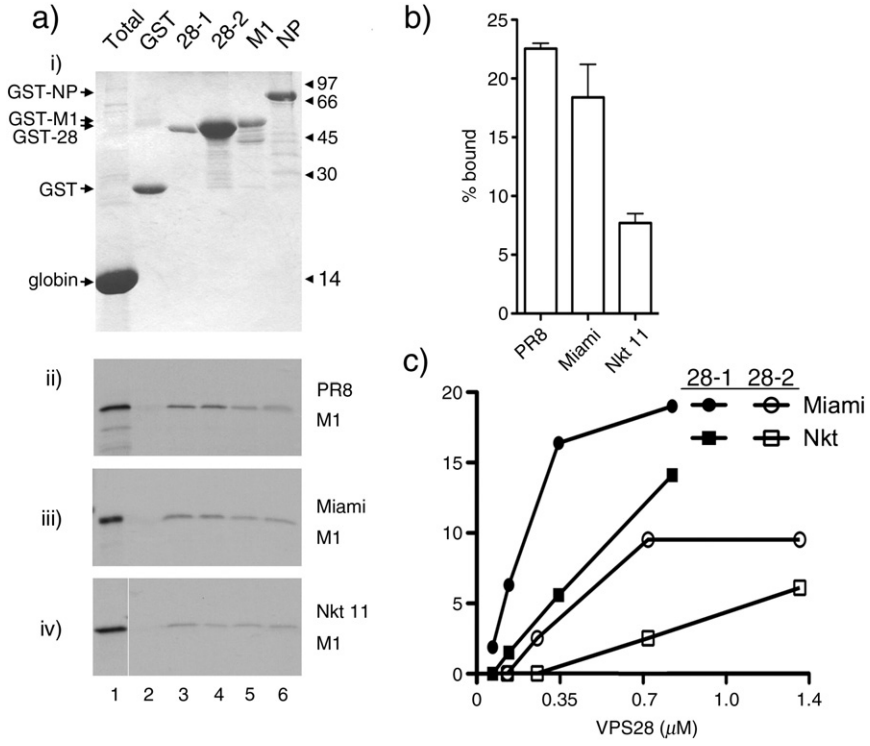

Fig. 1. Interaction of M1 and VPS28 *in vitro*. (a) Radiolabelled *in vitro* translated PR8, Miami or Nkt 11 M1 proteins were analysed by SDS-PAGE and (i) Coomassie blue staining (from the PR8 M1 experiment) or (ii) autoradiography before (Total; note the predominant polypeptide species in unfractionated reticulocyte lysate is globin) or after binding to the indicated GST fusion proteins (28-1; VPS28-1, 28-2; VPS28-2, M1; GST-M1, NP; GST-NP) immobilised on glutathione sepharose. (b, c) The amounts of radiolabelled *in vitro* translated M1 from the indicated strains of virus that bound to (b) 6 μg of GST-VPS28-1 or (c) the indicated amounts of GST-VPS28-1 or GST-VPS28-2 were determined by densitometry and plotted as the % of the input material. The mean and range of two independent experiments is plotted in (b) while the results of a single experiment are shown in (c).

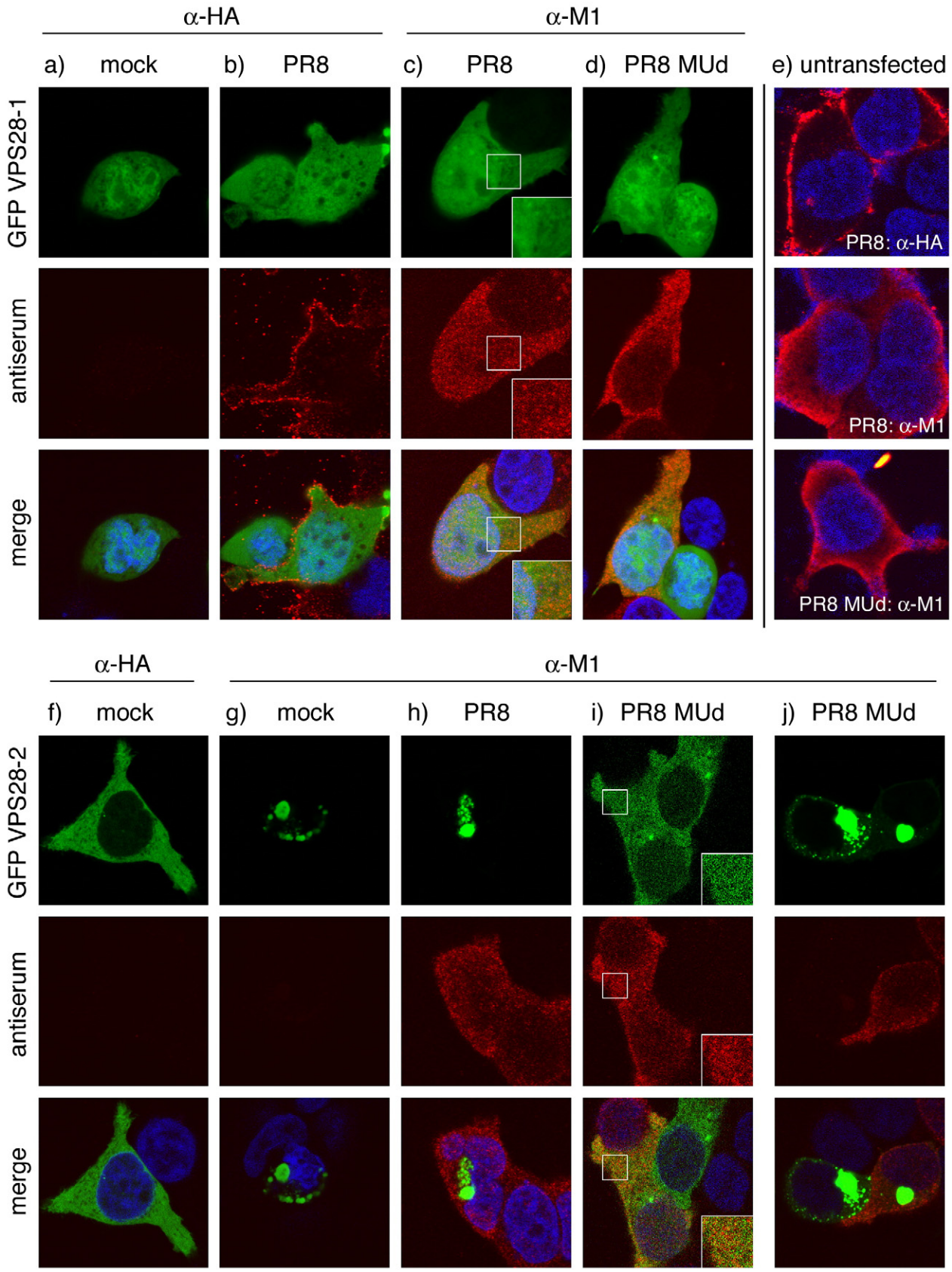

Fig. 2. Intracellular localisation of VPS28. 293T cells were transfected (or (e), mock transfected) with plasmids encoding (a–d) GFP-VPS28-1 or (f–j) GFP-VPS28-2 and 18 h later (a, f, g) mock infected or (b–e, h–j) infected at an MOI of 2 with influenza viruses as labelled. At 8 h p.i. cells were fixed, permeabilised, stained with the indicated antisera and DAPI and imaged by confocal microscopy. The main images represent a 39.5 μm square window. Insets show higher magnification views of the areas indicated by white boxes.

their ability to bind radiolabelled *in vitro* translated PR8 M1 in "pull-down" assays, both fusion proteins but not GST alone bound M1 with reasonable efficiency (Fig. 1a, panel ii; compare lanes 2–4). Furthermore, the *in vitro* translated M1 bound to GST tagged VPS28-1 with greater apparent affinity than the positive controls, GST-M1 and GST-NP (Fig. 1a; compare lanes 3, 5 and 6). Having reproduced an M1–VPS28 interaction *in vitro*, we next tested whether M1 polypeptides from filamentous and non-filamentous strains of virus differed in their binding activity. As reagents, we had available the M1 genes from two strains of equine influenza (A/eq/Newmarket/11/03 (Nkt 11) and A/eq/Miami/63 (Miami)) for which reverse-genetic analyses had established that they determined the respective filamentous and non-filamentous nature of the viruses (DE, EM and PD, manuscript in preparation and see Fig. 6). Similar amounts of the Miami and Nkt 11 matrix proteins bound to PR8 GST-M1 and GST-NP as the homologous interaction (Fig. 1a, panels ii–iv, lanes 5 and 6). However, while the equine virus matrix proteins also bound to the GST-VPS28 polypeptides, the interaction of the Nkt 11 protein was noticeably reduced (lanes 3 and 4). In confirmation of this, when replicate experiments were quantified by densitometry, the M1 proteins from the non-filamentous PR8 and Miami strains bound to VPS28-1 with similar efficiency, with 0.7 μM VPS28 retaining around 20% of the *in vitro* translated M1 (Fig. 1b). In contrast, the M1 protein from the filamentous Nkt 11 virus bound significantly less well, with less than 10% of the input material being retained. To examine this in more detail, we titrated the binding activity of both VPS28 isoforms for the equine influenza M1 polypeptides. Miami M1 bound to either isoform of VPS28 better than the Nkt 11 M1 at all VPS28 concentrations tested, while VPS28-1 showed higher affinity for either M1 polypeptide than VPS28-2 (Fig. 1c). Thus in corroboration of the findings of Hui et al. (2006a), we find evidence for an interaction between influenza A M1 and VPS28 *in vitro*. Furthermore, this interaction shows virus strain and isoform-dependent variation in strength.

Expression of HIV-1 Gag or Ebola virus VP40 induces the relocalisation of VPS28-1 to the plasma membrane (Martin-Serrano et al., 2003b; Silvestri et al., 2007). To further examine the role of VPS28 in influenza infection we next investigated whether it colocalised with the viral structural proteins and if its localisation changed in response to infection. 293T cells were transfected with plasmids encoding GFP-tagged VPS28-1 or -2, then infected or mock infected with either non-filamentous (PR8) or filamentous (PR8 MUd; Noton et al., 2007) strains of influenza virus. At 8 h post infection, cells were fixed and the localisation of the fluorescently tagged VPS28 proteins as well as influenza proteins stained by immunofluorescence were visualised by confocal microscopy. No antibody-dependent signal was seen from mock infected cells stained with anti-HA (Figs. 2a, f) or M1 antibodies (Fig. 2g). In most mock infected cells, GFP-VPS28-1 localised diffusely throughout the cell, including both cytoplasm and nucleus (Fig. 2a), in agreement with previously published data examining the intracellular localisation of recombinant myc- or CFP-tagged VPS28 proteins (Bishop and Woodman, 2001; Martin-Serrano et al., 2003b) as well as untagged VPS28 (Silvestri et al., 2007). In a minority of cells, bright cytoplasmic accumulations several microns across were observed (data not shown, but see Fig. 3), reminiscent of the swollen endosomes observed after expression of dominant negative versions of the AAA-ATPase VPS4 (Bishop and Woodman, 2000; Fujita et al., 2003); see also Figs 5 and 6. VPS28-1 localisation was not discernibly altered by influenza virus infection, whether with the non-filamentous PR8 or filamentous PR8 MUd strains of virus (Figs. 2a–d). As expected, the viral HA protein localised at the plasma membrane in cells infected with PR8; no specific colocalisation with the GFP VPS28-1 protein was observed (Fig. 2b). HA

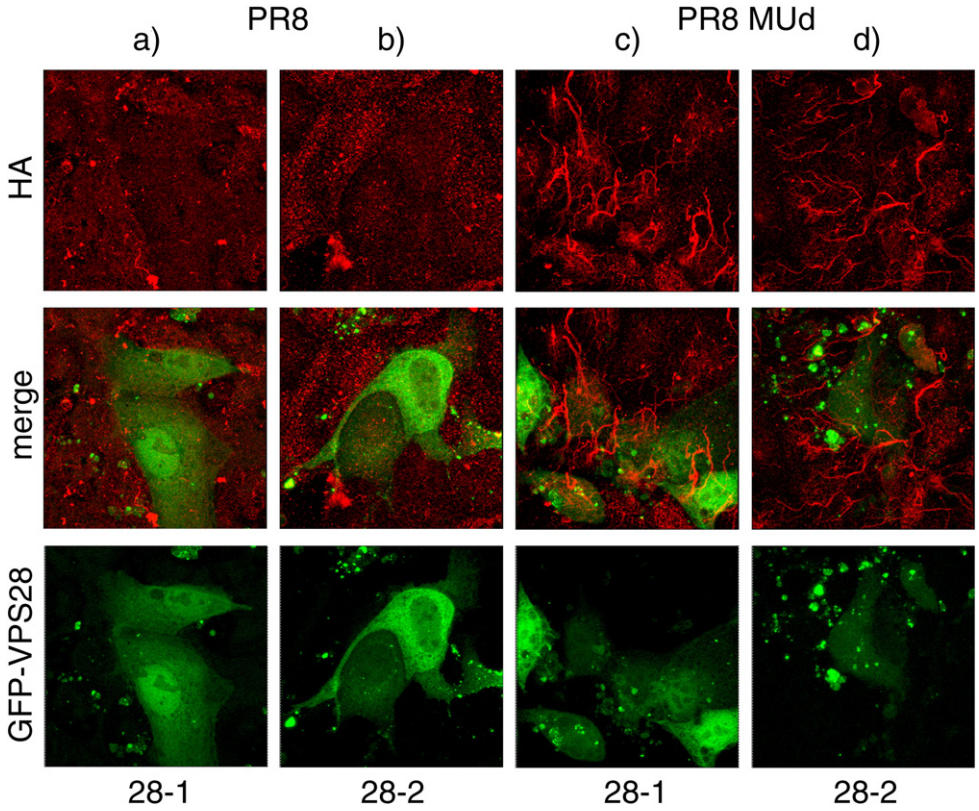

Fig. 3. Effect of GFP-VPS28 overexpression on viral filament production. MDCK cells were transfected with plasmids encoding GFP-VPS28-1 (a, c) or 28-2 (b, d) and 18 h later infected with (a, b) PR8 or (c, d) PR8 MUd virus at an MOI of 5. Cells were fixed after an overnight incubation and surface HA stained with anti-whole PR8 virus serum before imaging by confocal microscopy. Images represent a 39.5 μm square window and are maximum intensity projections summing multiple Z-axis planes of focus across the depth of the cells.

localisation in cells over-expressing GFP VPS28-1 did not appear to differ from that observed in cells infected with PR8 MUd (data not shown), or in untransfected cells (Fig. 2e). Similarly, M1 protein from both PR8 and PR8 MUd was found throughout the cell though predominantly in the cytoplasm in a manner that did not appreciably differ between GFP VPS28-1-transfected cells and untransfected cells (Figs. 2c–e). While low magnification merged images of superinfected GFP VPS28-1 transfections appeared to reveal a degree of colocalisation between VPS28-1 and M1 proteins resident in the cytoplasm and nucleus, inspection of higher magnification images revealed that the M1 staining was more granular than GFP VPS28-1 and the degree of true colocalisation was poor (Fig. 2c, inset).

In uninfected cells transfected with GFP VPS28-2, two common patterns of intracellular localisation were seen. In around half the cells, the protein exhibited a diffuse cytoplasmic localisation with exclusion from the nucleus (Fig. 2f), but large numbers of cells also exhibited large cytoplasmic accumulations (Fig. 2g). These patterns were also seen at similar frequencies in infected cells (Figs. 2h–j). Furthermore, in neither case, did M1 show substantial amounts of colocalisation with the fluorescent VPS28-2. High magnification examination of infected cells containing diffusely localised VPS28-2 showed that similarly to the case with VPS28-1, the cytoplasmic puncta of M1 and VPS28-2 did not show a strong correlation (Fig. 2i, inset). Neither M1 (Figs. 2h, j) nor HA (data not shown) appeared to be recruited to the aggregates present in many cells over-expressing VPS28-2, suggesting that the HA and M1 proteins are trafficked to their normal cellular destinations even in the presence of aggregated VPS28-2 protein. Overall therefore, despite *in vitro* evidence for an M1–VPS28 interaction, the polypeptides did not obviously influence each other's localisation in infected cells. However, they were both clearly cytosolic, and so low levels of colocalisation may be present.

Role of VPS28 in influenza A budding

Our hypothesis that the strength of the M1–VPS28 interaction determines the efficiency with which virus buds and hence determines whether spherical or filamentous particles are formed predicts that overexpression of VPS28 might affect the budding morphology of the virus. Simply, supplying additional VPS28 might bias budding towards production of spherical particles. Alternatively, as overexpression of some fluorescently tagged ESCRT proteins has been shown to have trans-dominant inhibitory effects on viral budding (Martin-Serrano et al., 2003a; von Schwedler et al., 2003), it was possible that the opposite effect could be obtained, biasing virus budding towards the production of filaments. To test these possibilities, MDCK cells were transfected with GFP-VPS28 proteins, superinfected with filamentous PR8 MUd or non-filamentous PR8 viruses and surface HA localisation monitored by immunofluoresence. In cells infected with non-filamentous strains of virus, HA normally forms a stippled pattern across the apical plasma membrane, whereas HA in viral filaments forms readily visible micrometer length structures (Roberts and Compans, 1998; Simpson-Holley et al., 2002). However, cell surface HA remained in a stippled pattern in VPS28 transfected cells infected with PR8 virus, even in cells where the foci of overexpressed VPS28 polypeptide suggested that MVB trafficking was disrupted (Figs. 3a, b). Similarly, PR8 MUd infected cells produced abundant filaments regardless of transfection status, whether the VPS28 polypeptide was diffusely localised or aggregated, or whether isoform 1 or 2 was used (Figs. 3c, d). Thus surface HA localisation and viral filament formation is apparently independent of GFP-VPS28 overexpression.

As the above data relied on overexpression of GFP-tagged constructs, we next explored the role of endogenous VPS28. To examine further any role VPS28 might play in influenza infection, siRNA treatment was used to knock down endogenous VPS28 expression and virus replication monitored. Triplicate wells of 293T cells were transfected with siRNA sequences directed against VPS28, or, as controls, with siRNAs targeted against the cellular housekeeping gene glyceraldehyde-3-phosphate dehydrogenase (GAPDH), a pool of non-targeting siRNA sequences, or mock transfected without siRNA. The cells were infected with PR8 virus 48 h post transfection and a further 24 h later replicated virus was collected and titred by plaque assay while cell lysates were harvested for western blot analysis of VPS28 levels. A polypeptide with the same apparent molecular weight as purified recombinant VPS28 was seen in all samples from control cells (Fig. 4a, lanes 2, 4 and 6) that was much reduced in quantity in cells treated with siRNA against VPS28 (lanes 3, 5 and 7), indicating successful knockdown of endogenous VPS28-1. The amount of VPS28-1 protein detected by western blotting was quantified by densitometry and normalised to tubulin levels, revealing over a 70% reduction in levels after siRNA treatment (Fig. 4b). However, both control and VPS28 siRNA-treated cells supported high levels of virus replication, producing titres of more than 10^7 PFU/ml, although the titres from the VPS28 depleted cells were marginally (less than 50%) lower (Fig. 4c). Similar results were obtained from a replicate experiment (data not shown) and overall, although virus replication was consistently around 2-fold lower in VPS28 depleted cells, the difference was not statistically significant (unpaired two tailed *t*-test, $N=6$). We conclude that influenza virus release either occurs in a VPS28-independent manner, or that only small quantities of VPS28 are needed. However, taken together with the fluorescence microscopy data showing no substantial

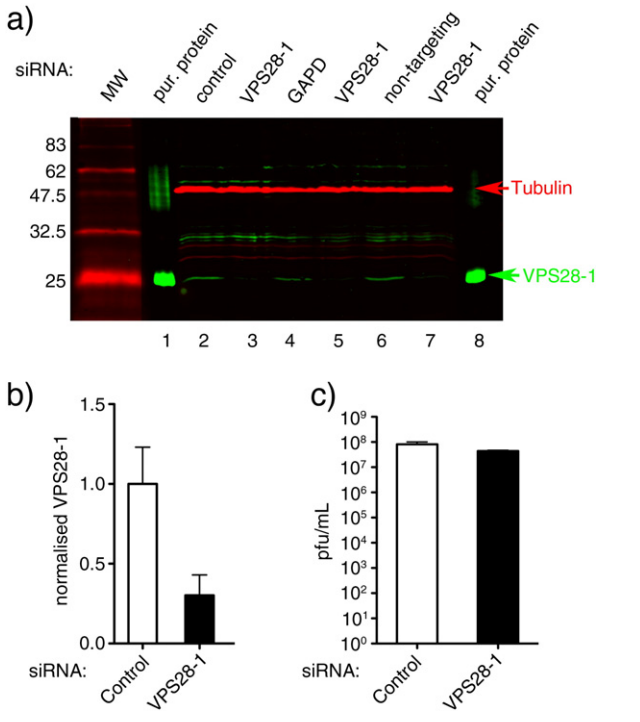

Fig. 4. Role of VPS28 in virus replication. 293T cells were transfected with siRNAs targeted against VPS28, the cellular housekeeping gene GAPDH, with a non-targeting pool, or mock transfected (−), followed 48 h later by infection with influenza A virus. (a) Cell lysates as well as aliquots of purified recombinant VPS28-1 were analysed 72 h post transfection by western blotting with antisera against VPS28-1 (green) or as a loading control, tubulin (red). MW; molecular mass markers (kDa). (b) VPS28 levels in (a) were quantified by densitometry and normalised to tubulin levels. Plotted values represent the mean + S.D. of three replicates of siRNA depletion of VPS28 relative to the mean + S.D. amounts obtained from the control treatments in (a). (c) Virus released by siRNA-treated cells was harvested at 24 h p.i. and titred by plaque assay. Values plotted represent the mean + S.D. as detailed in (b).

colocalisation between VPS28 and M1 (Fig. 2), or an effect of VPS28 overexpression on the morphology of virus budding (Fig. 3), no obvious role for VPS28 in influenza infection was apparent.

Role of VPS4 in influenza A budding

Since we found no obvious role for VPS28 in influenza virus budding, we next examined the role of downstream elements of the ESCRT pathway in this process. VPS4 plays a critical role in a final step of protein sorting into the intralumenal vesicles of MVBs; the dissociation of the ESCRT complexes from the membrane (Williams and Urbe, 2007). VPS4 is also required for successful budding of viruses containing all currently identified late domain motifs (Morita and Sundquist, 2004). Accordingly, microscopy was first used to test for colocalisation between VPS4 and viral proteins HA and M1 in the presence or absence of a functional ESCRT pathway. Stably transfected 293 cell lines were induced to express GFP-tagged fusion proteins of either WT VPS4 or a trans-dominant ATPase defective VPS4 EQ mutant by the addition of ponasterone A (Crump et al., 2007) and after an overnight incubation, infected (or mock infected) with PR8 virus. At 8 h post infection cells were fixed and stained for HA or M1. In mock infected cells, the fluorescently tagged WT VPS4 protein showed a diffuse, mostly cytoplasmic localisation (Fig. 5a), while the dominant negative mutant, VPS4 EQ, formed the characteristic bright cytoplasmic aggregates of protein seen by others (Fig. 5b) (Bishop and Woodman, 2000; Crump et al., 2007; Fujita et al., 2003). Mock infected cells did not stain strongly with either anti-M1 or anti-HA sera (Figs. 5a and b respectively). Infection with PR8 virus did not result in appreciable redistribution of either WT or EQ VPS4 with the functional version of the protein remaining in a diffuse, largely cytoplasmic staining pattern while the trans-dominant inhibitor still formed prominent cytoplasmic aggregates (Figs. 5c–f). Influenza M1 also showed the expected cytoplasmic staining pattern in cells expressing the WT GFP-VPS4 fusion polypeptide and although some apparent colocalisation could be seen (Fig. 5c), inspection of higher power images showed that as with VPS28 (Fig. 2), this primarily reflected the fact that both polypeptides were largely cytoplasmic rather than true colocalisation of discrete fluorescent foci (data not shown). Similarly, while in some cells, a superficial level of WT VPS4-HA colocalisation in the peri-nuclear region was apparent, inspection of higher magnification images revealed that the two proteins were localised in juxtaposed structures rather than displaying convincing coincidence (Fig. 5e, inset). Furthermore, the localisation of M1 and HA was unaltered in cells expressing the dominant negative VPS4 EQ protein, with no visible recruitment of either viral polypeptide to the disrupted MVBs (Figs. 5d, f). A similar outcome was obtained when the filamentous PR8 MUd virus was used (data not shown). Thus, overexpression of the wildtype or dominant negative VPS4 protein did not perturb viral protein localisation or trafficking. Since expression of polypeptides from ESCRT-dependent viruses often (though not always) results in relocalisation of ESCRT components and conversely, these viral polypeptides relocalise in response to disruption of the ESCRT pathway (Calistri et al., 2007; Martin-Serrano et al., 2001, 2003b; Medina et al., 2005; Silvestri et al., 2007; Welsch et al., 2006), the failure to observe similar outcomes with the major influenza virus structural polypeptides does not support the hypothesis that influenza virus budding involves the ESCRT pathway.

As we had originally hypothesised that modulation of the interaction between virus and the cellular ESCRT pathway determined whether or not virus budding produced filamentous particles, MDCK cells were transfected with plasmids expressing WT or EQ GFP-tagged VPS4, superinfected with a non-filamentous reassortant PR8 virus containing segment 7 from A/eq/Miami/63

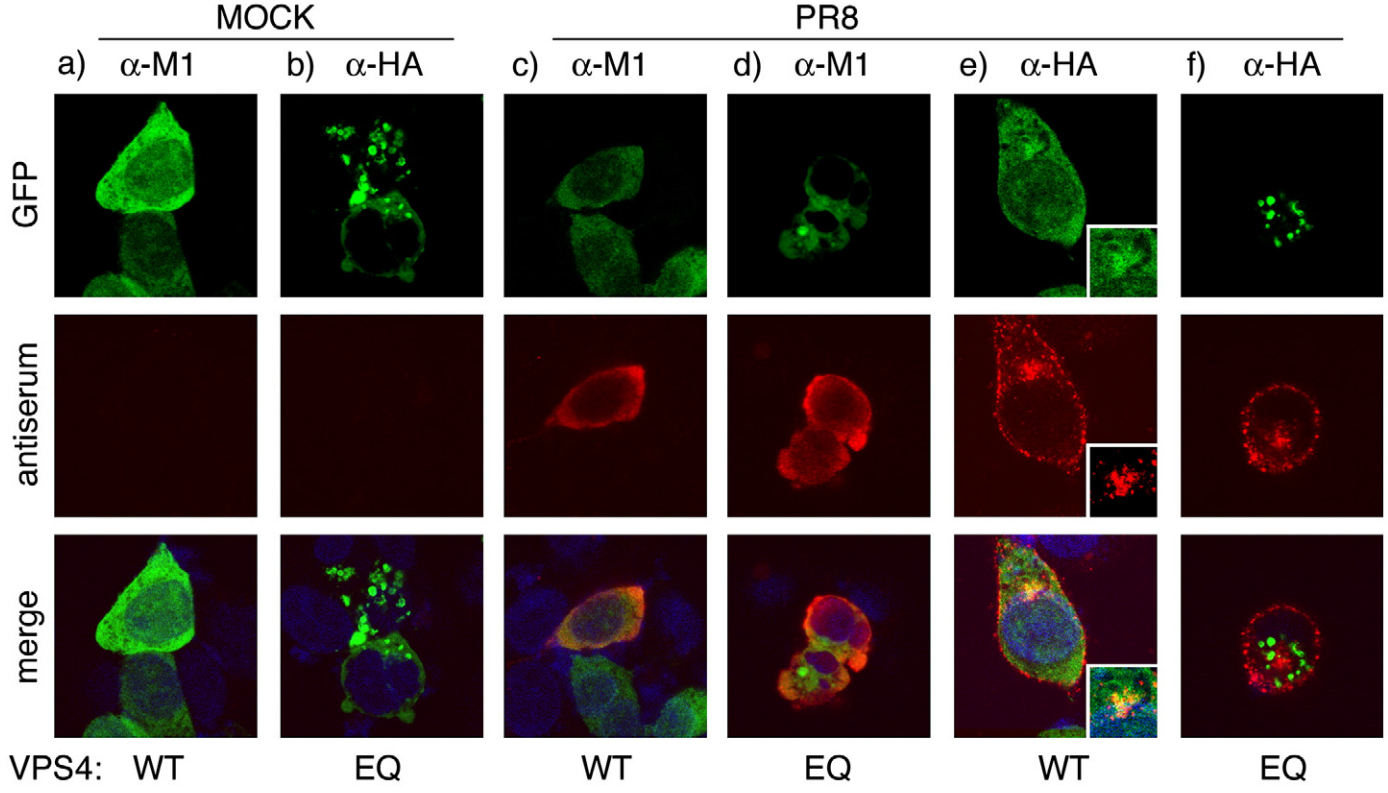

Fig. 5. Intracellular localisation of VPS4 and influenza polypeptides. 293 cell lines expressing WT or EQ mutant VPS4 proteins fused to GFP were infected (c–f) or mock infected (a, b) with PR8 virus at an MOI of 2 as labelled, fixed and stained for the indicated viral antigens and with DAPI at 8 h.p.i.

(PR8-Miami) or a filamentous reassortant containing segment 7 from A/eq/Newmarket/11/03 (PR8-Nkt 11) and stained for cell surface HA in order to visualise filament formation. In cells over-expressing WT VPS4, HA exhibited the expected localisation patterns for a non-filamentous virus of punctate accumulation at the apical cell surface in PR8-Miami infection (Fig. 6a) and long filamentous particles extruding from the cell membrane in PR8-Nkt11 infection (Fig. 6c). These patterns were not changed by overexpression of the dominant negative VPS4 protein, with cells infected with PR8-Miami exhibiting the same surface accumulation seen in cells expressing the WT VPS4 protein (Fig. 6b) while cells infected with PR8-Nkt11 still produced long filamentous structures (Fig. 6d). Thus, overexpression of dominant negative VPS4 does not induce the normally spherical PR8-Miami virus to produce filamentous particles, while overexpression of WT VPS4 did not prevent PR8-Nkt11 from forming filamentous particles.

The ability of the viral M1 and HA proteins to maintain their normal localisation patterns in the absence of a functional ESCRT pathway as well as the maintenance of filament formation suggested that influenza budding itself may be VPS4 independent. To test this hypothesis further, we examined the ability of the VPS4 and VPS4 EQ cell lines to support influenza virus replication. 18 h post induction, cells were infected with either PR8, the filamentous influenza virus strains PR8 MUd or A/Udorn/72 (Udorn), or herpes simplex virus type I (HSV). HSV was used as a positive control, as it is known to require a functional VPS4 protein in order to undergo final envelopment (Crump et al., 2007). Induction of the GFP VPS4 proteins was verified by observing levels of GFP signal at 18 h post induction (data not shown). At 24 h p.i., viral supernatants were harvested and titred. In cells expressing WT VPS4, HSV replicated to high titres of greater than 10^7 pfu/ml. However, as expected (Crump et al., 2007) cells expressing the non-functional VPS4 EQ protein produced nearly 400-fold less virus (Fig. 7a), thus confirming that the VPS4 EQ cell line was behaving as expected. Influenza PR8 virus also replicated well in WT GFP-VPS4 expressing cells, producing on average 2×10^7 pfu/ml, while PR8 MUd and Udorn replicated rather less well, producing titres of only around 10^5 pfu/ml. Reduced growth in tissue culture of filamentous influenza viruses is a feature that has been seen before (Roberts and Compans, 1998). However, similar titres of all three viruses were produced from VPS4 EQ cell lines, and statistical analysis (unpaired *t*-test) showed no significant difference between the titres produced in VPS4 WT as compared to VPS4 EQ cells (Fig. 7a). As these results examined the release of virus from a single round of high multiplicity infection, we next examined the kinetics of viral growth in low multiplicity multi-cycle infections over a longer time course. Under these conditions, HSV replication was effectively blocked in cells expressing the VPS4 EQ protein (Fig. 7b). In contrast, both filamentous Udorn and non-filamentous PR8 viruses replicated to titres of more than 10^6 PFU/ml in both cell lines (Fig. 7c). At most time points with both influenza viruses, titres released from cells expressing the VPS4 EQ protein were generally slightly lower than from the WT cells. This was most noticeable at 24 h.p.i. in Udorn-infected cells, where an approximately ten-fold reduction in titre released was apparent. However, the final end point titres of both viruses in both cell types were very similar. Bearing in mind the substantial cytotoxicity of the VPS4 EQ protein and contrasted with the almost complete failure of HSV to replicate, this shows at best only a minor role for the ESCRT pathway in influenza virus budding. Overall, from these data, as well as the preceding experiments, we conclude that influenza

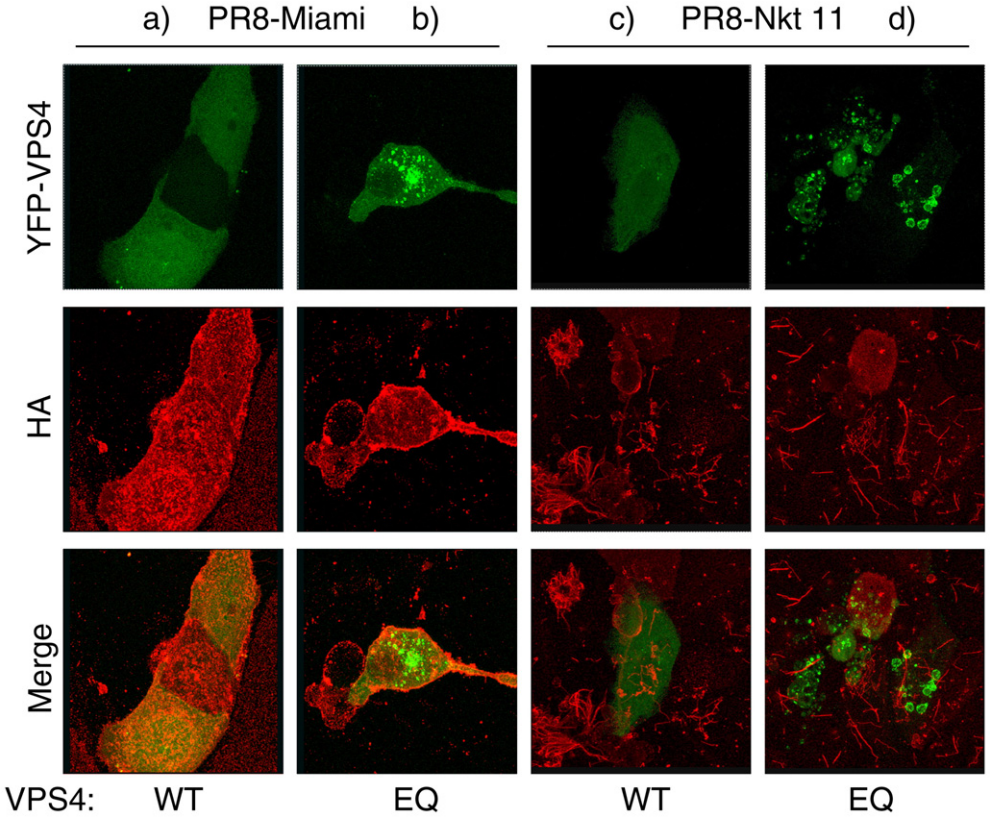

Fig. 6. Effect of YFP-VPS4 overexpression on viral filament production. MDCK cells were transfected with plasmids encoding WT YFP-VPS4 (a, c) or the trans-dominant YFP-VPS4 EQ mutant (b, d), incubated overnight and then infected with (a, b) PR8-Miami or (c, d) PR8-Nkt 11 virus at an MOI of 5. Cells were fixed after an overnight incubation and surface HA stained with anti-PR8 serum before imaging by confocal microscopy. Images represent a 39.5 μm square window and are maximum intensity projections summing multiple *Z*-axis planes of focus across the depth of the cells.

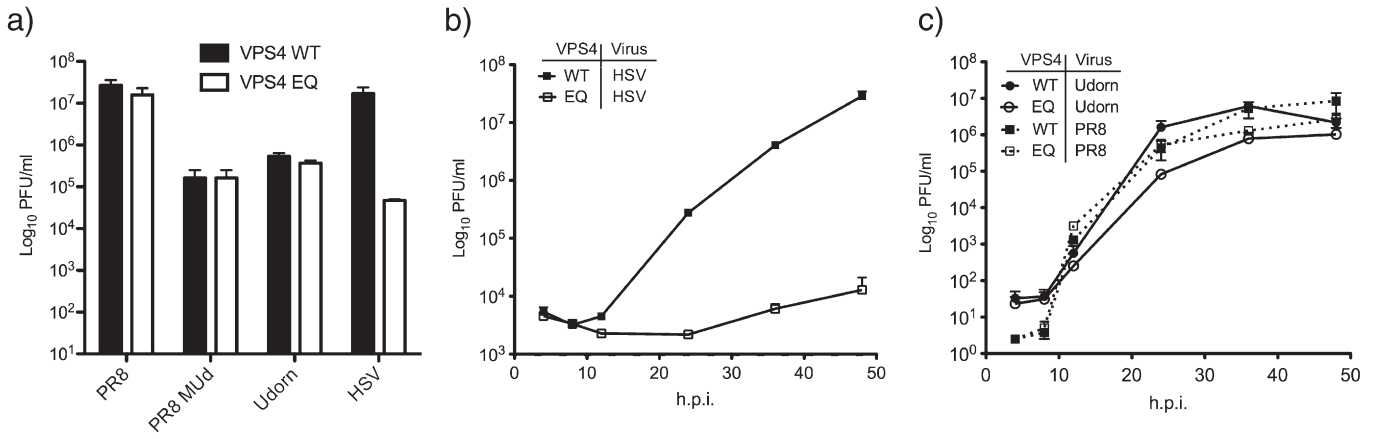

Fig. 7. Effect of the trans-dominant VPS4 EQ mutant on influenza virus and HSV release. 293 cell lines expressing WT or EQ mutant VPS4 proteins fused to GFP were infected with PR8, Udorn or PR8 MUd influenza viruses at (a) an MOI of 2 or with HSV at an MOI of 5. 24 h p.i., the titres of released virus were determined by plaque assay. Plotted values represent the mean and range of two (PR8 MUd, Udorn) or three (PR8) independent experiments or two replicates within a single experiment (HSV). (b, c) Cells were infected with PR8 or Udorn influenza viruses at an MOI of 0.005 (c) or with HSV at an MOI of 0.05 (b). The titres of virus released at the indicated h.p.i. were determined by plaque assay. The mean and range of two replicate experiments are plotted for PR8 and HSV while the mean ± SEM of four replicates from two independent experiments are plotted for Udorn virus.

virus assembly and budding, whether of spherical or filamentous particles, occurs independently of the ESCRT pathway.

Discussion

Previous reports suggested that the influenza A virus matrix protein contained a late domain that interacted with VPS28, a cellular protein in the ESCRT-I complex (Hui et al., 2003, 2006a). This prompted us to hypothesise that influenza particle shape might be controlled by the strength of the interaction between the M1 protein and the ESCRT machinery. In support of this, we found that *in vitro*, the matrix proteins from two strains of non-filamentous influenza virus bound well to VPS28-1 while an M1 polypeptide from a filamentous strain of virus bound less strongly (Fig. 1). However, while our studies were in progress, the Hui papers were retracted when the supposedly viable late domain mutants were found to contain wildtype virus genomes (Hui et al., 2006b), leaving the fundamental mechanism of influenza virus budding unclear. This accords with our own data, in that we were unable to rescue viruses with alternative 'late domain' sequences (data not shown). Subsequent work showed that expression of a variety of dominant negative VPS4 proteins had no effect on influenza VLP release (Chen et al., 2007), arguing against a role for the ESCRT system. However, as we had found independent support for an interaction between M1 and the VPS28 subunit of the ESCRT-I complex, and the role of VPS4 in the morphogenesis and budding of authentic influenza virus particles (as opposed to recombinant VLPs) had not been explored, there was a clear rationale for studying the participation of the ESCRT pathway in influenza budding in greater detail.

Despite the positive finding of an interaction between M1 and VPS28, the rest of our findings were largely negative. Confocal microscopy of infected cells found no great degree of colocalisation or redistribution between the major influenza virus structural proteins and the ESCRT components under study. Overexpression of either VPS28 isoform, VPS4 or VPS4 EQ had no visible effect on the production of filamentous viral particles. SiRNA-mediated depletion of endogenous VPS28 had no significant effect on the titre of viral replication. Infection of stable cell lines expressing WT or trans-dominant VPS4 with either spherical or filamentous influenza viruses showed that viral output was not dependent on the presence of a functional VPS4 protein. Overall therefore, in agreement with the conclusions of Chen et al. (2007) regarding the lack of involvement of VPS4 in influenza VLP production, we find no obvious role for the ESCRT pathway in the release of authentic influenza virus particles, whether spherical or filamentous.

However, several aspects of these negative findings deserve further consideration. Little characterisation of the VPS28-2 isoform has been reported, beyond the sequence of its encoding mRNA and the notation that it is a minor isoform (NCBI entry NM_016208). Consistent with this, we were unable to detect a polypeptide with the expected electrophoretic mobility for VPS28-2 in cell lysates (Fig. 4). Although we have not formally tested it, we predict that our polyclonal anti-VPS28-1 serum would cross-react with VPS28-2 as the proteins share 183 common amino-acids out of 221/233 residues in total. However, characterisation of GFP-tagged VPS28-1 and VPS28-2 showed that intracellular localisation of the proteins differed between isoforms (Fig. 2). That observed for GFP VPS28-1 was similar to the pattern reported for tagged and untagged forms of VPS28 (Bishop and Woodman, 2001; Martin-Serrano et al., 2003b; Silvestri et al., 2007), but the distribution of VPS28-2 was noticeably different both for its exclusion from the nucleus and its increased propensity to form large cytoplasmic protein aggregates. It is difficult to say whether the aggregates are indicative of the endogenous protein localisation. On one hand, it is possible that overexpression (perhaps combined with fusion of the GFP fluorophore), is interfering with normal VPS28-2 function to the extent that the protein has become trans-dominant and (much like VPS4 EQ), is inducing the formation of enlarged endosomes and disrupting the ESCRT pathway. However, VPS28-2 differs from VPS28-1 in lacking the C-terminal 38 amino-acids present in the dominant isoform and having a larger, alternative 50 residue tail. The C-terminal domain of VPS28-1 is involved in interactions with the downstream ESCRT II complex via VPS20 (Pineda-Molina et al., 2006; Teo et al., 2006) so it is therefore possible that endogenous VPS28-2 has inhibitory properties in the ESCRT pathway.

Depletion of VPS28-1 to roughly 30% of endogenous levels had no significant effect on influenza virus replication in experiments we performed (Fig. 4). Additionally, we predict that the siRNAs used would knock down expression of VPS28-2 as well, due to the sequence similarity between the two isoforms. Two independent siRNA experiments, each containing three replicates, were carried out. Statistical analysis of data from the amalgamated experiments revealed no significant difference in viral titre from cells depleted of VPS28 and those receiving control treatments. While we cannot rule out the possibility that more efficient knockdown of VPS28 expression would reveal an inhibitory effect on influenza virus replication, taken together with the lack of effect of GFP-VPS28 overexpression on filamentous virus production and the low degree of colocalisation

between M1 and VPS28 in infected cells (Figs. 2 and 3), this suggests that overall, VPS28 is not critical for virus replication in cultured cells. The question therefore arises as to the significance of the interaction we observe between the two proteins (Fig. 1). A negative interpretation would be that it is simply an *in vitro* association between two proteins with overall opposing charges (M1 pI = 9.4 versus VPS28-1 pI = 5.5). Consistent with a charge-based interaction, VPS28-2 has a much more basic C-terminal domain than VPS28-1 and it bound M1 markedly less well (Fig. 1c). On the other hand, there are only 4 amino-acid differences between the M1 proteins of Miami and Nkt11 viruses (DE, PD; unpublished data) with no resulting charge differential, so the lower binding affinity of the Nkt11 M1 protein argues for a degree of specificity to the interaction. A more interesting hypothesis therefore, is that the *in vitro* interaction reflects a viral adaptation of little significance to replication in tissue culture but potentially greater significance in the multicellular host. Given the lack of evidence for the involvement of the ESCRT pathway in influenza virus budding (Chen et al., 2007; this study), we speculate that the M1–VPS28 interaction functions in another pathway than MVB sorting. There is evidence for additional roles of ESCRT proteins in cellular processes such as mRNA transport, signalling, autophagy and cytokinesis (Carlton and Martin-Serrano, 2007; Giebel and Wodarz, 2006; Pilecka et al., 2007; Rusten and Simonsen, 2008; Sevrioukov et al., 2005), so this is not implausible.

As the ESCRT system plays a crucial role in the budding of many viruses, it is clearly useful to identify those, such as influenza, that are able to bud independently of this pathway. The search for other cellular proteins that can facilitate this final pinching off process is an important one for both cell biologists and virologists. Although influenza does not appear to use the ESCRT system, it is likely that there are other cellular proteins involved. Proteins containing Bin-Amphiphysin-Rvs (BAR) domains have been implicated in inducing membrane curvature during viral budding (Wang et al., 2003). Additionally, recent computer modelling simulations suggest that spontaneous vesicle formation can occur. In this scenario, protein aggregation at specific sites on the plasma membrane and a hydrophilic attraction between proteins and their immediate lipid surroundings is able to drive membrane curvature in the absence of inter-protein interactions (Reynwar et al., 2007). However, membrane curvature alone is not enough to account for the formation of completely budded vesicles, indicating that as-of-yet unidentified cellular proteins might be involved in the final steps of the budding process filled for other viruses by VPS4 (Chen and Lamb, 2008). Respiratory syncytial virus also buds through a VPS4-independent pathway and it was recently shown that here, budding is controlled by Rab11-FIP2 (Utley et al., 2008). It is hoped that advances in mass spectrometry and large-scale proteomic screening will be able to identify possible cellular cofactors for influenza budding.

Materials and methods

Cells, viruses, plasmids and antisera

Human embryonic kidney 293T cell line, Madin–Darby Canine Kidney (MDCK) cells and African green monkey kidney Vero cells were cultured as previously described (Carrasco et al., 2004; Crump et al., 2007). 293 cell lines that inducibly express GFP-VPS4A and GFP-VPS4EQ proteins (Crump et al., 2007) were maintained in medium supplemented with 0.2 mg/ml Zeocin (Invitrogen) and 0.4 mg/mL G418 (PAA Laboratories GmbH). Expression of the GFP VPS4 proteins was induced by adding 2.5 μg/ml Ponasterone A (Invitrogen) and incubating for ~18 h. Cells were transfected with plasmids using Lipofectin or Lipofectamine 2000 (Invitrogen) according to the manufacturer's instructions. For transfection of siRNAs, 293T cells (plated in a 6 well plate at 5×10^5 cells/well in 2 ml antibiotic free media) were transfected approximately 18 h after seeding using DharmaFECT transfection reagent (Dharmacon, 4 μl/well) to final siRNA concentration of 0.1 μM.

The Cambridge lineage of PR8 virus was propagated in embryonated eggs as previously described (Elton et al., 2001), while for experiments involving the growth of virus in cultured cells, A/Udorn/72 (Simpson-Holley et al., 2002) or an MDCK-adapted version of PR8 rescued from plasmids (de Wit et al., 2004) and grown in MDCK cells was used. A filamentous variant of PR8 containing segment 7 from A/Udorn/72 (PR8 MUd) has been previously described (Noton et al., 2007). Similar reverse-genetics strategies were used to create another filamentous PR8 virus containing segment 7 from A/eq/Newmarket/11/02 (PR8-Nkt11) as well as a non-filamentous reassortant (PR8-Miami) with segment 7 from A/eq/Miami/63). HSV type I strain SC16 was propagated in Vero cells. For influenza virus infections (except multi-cycle growth curves), virus was adsorbed to cells for 30 min in Optimem medium at 37 °C before a 1 minute acid wash (10 mM HCl, 150 mM NaCl, pH 3) to remove residual inoculum followed by 3 washes with warm PBS and incubation in Optimem supplemented with 1 μg/ml trypsin. HSV infections were performed similarly except that medium containing serum was used and trypsin was omitted. Influenza viruses were titred by plaque assay in MDCK cells (Matrosovich et al., 2006) while HSV was titred by plaque assay in Vero cells. For multi-cycle growth curve infections, influenza virus was adsorbed to cells for 1 h in serum free media, then overlayed with serum free media containing 1 μg/ml trypsin and 0.14% BSA.

Bacterial expression plasmids pGEX-NP and pGEX-M1 that express PR8 NP or M1 respectively as GST fusion proteins have been previously described (Digard et al., 1999; Noton et al., 2007). VPS28 variant 1 (VPS28-1) and variant 2 (VPS28-2) were amplified by PCR from IMAGE clones 3535787 and 5741129, respectively, and subcloned into pGEX4T-1 (GE Healthcare) for expression of GST fusion proteins; or into pEGFP-C1 (Clontech) for the expression of N-terminally GFP-tagged proteins in mammalian cells. Plasmids encoding yellow fluorescent protein (YFP)-tagged WT and dominant negative E228Q (EQ) VPS4 proteins were generously supplied by Dr Juan Martin-Serrano et al. (2003a).

Rabbit polyclonal antisera to whole PR8 virus and PR8 M1 have been described previously (Amorim et al., 2007). Clone 6F6 anti-PR8 HA mouse monoclonal antibody was a gift from Dr Philip Stevenson. To generate an anti-VPS28 serum, rabbits were immunised twice with GST-VPS28-1 fusion protein followed by a final boost with purified recombinant VPS28-1 protein.

Protein analyses

GST fusion proteins were expressed in *E. coli* and purified as previously described (Digard et al., 1999). To generate non-fused VPS28-1, 500 μl samples of dialysed protein (~0.1–0.2 mg) were adjusted to 2.5 mM $CaCl_2$ and cleaved with 3 U of thrombin at room temperature for 6 h. GST was removed by binding to glutathione sepharose, and protein-containing supernatant was lyophilised for rabbit immunisation or use as molecular weight marker.

Radiolabelled proteins were *in vitro* translated in rabbit reticulocyte and used in pull-down assays also as previously described (Elton et al., 1999). For western blotting, samples were separated by SDS-PAGE and transferred to nitrocellulose membranes according to standard procedures. Blots were developed using secondary antibodies conjugated to IR Dye 680 or 800 and imaged and quantified on a LiCor Biosciences Odyssey near-infrared imaging platform.

For fluorescent microscopy, cells were fixed with 4% formaldehyde and processed for immunocytochemistry as previously described (Elton et al., 2001; Simpson-Holley et al., 2002). Samples were imaged using a Leica TCS SP confocal microscope. Post-capture processing of

images to allow daylight visualisation and reproduction was applied equally to each experiment using Adobe Photoshop.

Acknowledgments

We thank Drs Juan Martin-Serrano, Philip Stevenson and Janet Daly for the gift of reagents. This work was supported by a grant from the BBSRC (no. S18874) to PD. EAB is supported by a scholarship from the Gates Cambridge Trust. SLN was supported by a BBSRC Committee studentship. CMC is a Royal Society University Research Fellow.

References

Amorim, M.J., Read, E.K., Dalton, R.M., Medcalf, L., Digard, P., 2007. Nuclear export of influenza A virus mRNAs requires ongoing RNA polymerase II activity. Traffic (Copenhagen, Denmark) 8 (1), 1–11.

Bankaitis, V.A., Johnson, L.M., Emr, S.D., 1986. Isolation of yeast mutants defective in protein targeting to the vacuole. Proc. Natl. Acad. Sci. U. S. A. 83 (23), 9075–9079.

Bieniasz, P.D., 2006. Late budding domains and host proteins in enveloped virus release. Virology 344 (1), 55–63.

Bishop, N., Woodman, P., 2000. ATPase-defective mammalian VPS4 localizes to aberrant endosomes and impairs cholesterol trafficking. Mol. Biol. Cell 11 (1), 227–239.

Bishop, N., Woodman, P., 2001. TSG101/mammalian VPS23 and mammalian VPS28 interact directly and are recruited to VPS4-induced endosomes. J. Biol. Chem. 276 (15), 11735–11742.

Bourmakina, S.V., Garcia-Sastre, A., 2003. Reverse genetics studies on the filamentous morphology of influenza A virus. J. Gen. Virol. 84 (Pt 3), 517–527.

Burleigh, L.M., Calder, L.J., Skehel, J.J., Steinhauer, D.A., 2005. Influenza a viruses with mutations in the m1 helix six domain display a wide variety of morphological phenotypes. J. Virol. 79 (2), 1262–1270.

Calistri, A., Sette, P., Salata, C., Cancellotti, E., Forghieri, C., Comin, A., Gottlinger, H., Campadelli-Fiume, G., Palu, G., Parolin, C., 2007. Intracellular trafficking and maturation of herpes simplex virus type 1 gB and virus egress require functional biogenesis of multivesicular bodies. J. Virol. 81 (20), 11468–11478.

Carlton, J.G., Martin-Serrano, J., 2007. Parallels between cytokinesis and retroviral budding: a role for the ESCRT machinery. Science (New York, N.Y.) 316 (5833), 1908–1912.

Carrasco, M., Amorim, M.J., Digard, P., 2004. Lipid raft-dependent targeting of the influenza A virus nucleoprotein to the apical plasma membrane. Traffic (Copenhagen, Denmark) 5 (12), 979–992.

Chen, B.J., Lamb, R.A., 2008. Mechanisms for enveloped virus budding: can some viruses do without an ESCRT? Virology 372 (2), 221–232.

Chen, B.J., Leser, G.P., Morita, E., Lamb, R.A., 2007. Influenza virus hemagglutinin and neuraminidase, but not the matrix protein, are required for assembly and budding of plasmid-derived virus-like particles. J. Virol. 81 (13), 7111–7123.

Cheung, T.K., Poon, L.L., 2007. Biology of influenza a virus. Ann. N.Y. Acad. Sci. 1102, 1–25.

Choppin, P.W., Tamm, I., 1960. Studies of two kinds of virus particles which comprise influenza A2 virus strains. II. Reactivity with virus inhibitors in normal sera. J. Exp. Med. 112, 921–944.

Crump, C.M., Yates, C., Minson, T., 2007. Herpes simplex virus type 1 cytoplasmic envelopment requires functional Vps4. J. Virol. 81 (14), 7380–7387.

de Wit, E., Spronken, M.I., Bestebroer, T.M., Rimmelzwaan, G.F., Osterhaus, A.D., Fouchier, R.A., 2004. Efficient generation and growth of influenza virus A/PR/8/34 from eight cDNA fragments. Virus Res. 103 (1–2), 155–161.

Digard, P., Elton, D., Bishop, K., Medcalf, E., Weeds, A., Pope, B., 1999. Modulation of nuclear localization of the influenza virus nucleoprotein through interaction with actin filaments. J. Virol. 73 (3), 2222–2231.

Elleman, C.J., Barclay, W.S., 2004. The M1 matrix protein controls the filamentous phenotype of influenza A virus. Virology 321 (1), 144–153.

Elton, D., Medcalf, E., Bishop, K., Digard, P., 1999. Oligomerization of the influenza virus nucleoprotein: identification of positive and negative sequence elements. Virology 260 (1), 190–200.

Elton, D., Simpson-Holley, M., Archer, K., Medcalf, L., Hallam, R., McCauley, J., Digard, P., 2001. Interaction of the influenza virus nucleoprotein with the cellular CRM1-mediated nuclear export pathway. J. Virol. 75 (1), 408–419.

Fujita, H., Yamanaka, M., Imamura, K., Tanaka, Y., Nara, A., Yoshimori, T., Yokota, S., Himeno, M., 2003. A dominant negative form of the AAA ATPase SKD1/VPS4 impairs membrane trafficking out of endosomal/lysosomal compartments: class E vps phenotype in mammalian cells. J. Cell. Sci. 116 (Pt 2), 401–414.

Garrus, J.E., von Schwedler, U.K., Pornillos, O.W., Morham, S.G., Zavitz, K.H., Wang, H.E., Wettstein, D.A., Stray, K.M., Cote, M., Rich, R.L., Myszka, D.G., Sundquist, W.I., 2001. Tsg101 and the vacuolar protein sorting pathway are essential for HIV-1 budding. Cell 107 (1), 55–65.

Giebel, B., Wodarz, A., 2006. Tumor suppressors: control of signaling by endocytosis. Curr. Biol. 16 (3), R91–R92.

Hui, E.K., Barman, S., Yang, T.Y., Nayak, D.P., 2003. Basic residues of the helix six domain of influenza virus M1 involved in nuclear translocation of M1 can be replaced by PTAP and YPDL late assembly domain motifs. J. Virol. 77 (12), 7078–7092.

Hui, E.K., Barman, S., Tang, D.H., France, B., Nayak, D.P., 2006a. YRKL sequence of influenza virus M1 functions as the L domain motif and interacts with VPS28 and Cdc42. J. Virol. 80 (5), 2291–2308.

Hui, E.K., Barman, S., Yang, T.Y., Tang, D.H., France, B., Nayak, D.P., 2006b. Retraction. J. Vir. 80 (20), 10289.

Jin, H., Leser, G.P., Zhang, J., Lamb, R.A., 1997. Influenza virus hemagglutinin and neuraminidase cytoplasmic tails control particle shape. EMBO J. 16 (6), 1236–1247.

Katzmann, D.J., Babst, M., Emr, S.D., 2001. Ubiquitin-dependent sorting into the multivesicular body pathway requires the function of a conserved endosomal protein sorting complex, ESCRT-I. Cell 106 (2), 145–155.

Kilbourne, E.D., Murphy, J.S., 1960. Genetic studies of influenza viruses. I. Viral morphology and growth capacity as exchangeable genetic traits. Rapid in ovo adaptation of early passage Asian strain isolates by combination with PR8. J. Exp. Med. 111, 387–406.

Martin-Serrano, J., Zang, T., Bieniasz, P.D., 2001. HIV-1 and Ebola virus encode small peptide motifs that recruit Tsg101 to sites of particle assembly to facilitate egress. Nat. Med. 7 (12), 1313–1319.

Martin-Serrano, J., Yarovoy, A., Perez-Caballero, D., Bieniasz, P.D., 2003a. Divergent retroviral late-budding domains recruit vacuolar protein sorting factors by using alternative adaptor proteins. Proc. Natl. Acad. Sci. U. S. A. 100 (21), 12414–12419.

Martin-Serrano, J., Zang, T., Bieniasz, P.D., 2003b. Role of ESCRT-I in retroviral budding. J. Virol. 77 (8), 4794–4804.

Matrosovich, M., Matrosovich, T., Garten, W., Klenk, H.D., 2006. New low-viscosity overlay medium for viral plaque assays. Virol. J. 3 (63).

Medina, G., Zhang, Y., Tang, Y., Gottwein, E., Vana, M.L., Bouamr, F., Leis, J., Carter, C.A., 2005. The functionally exchangeable L domains in RSV and HIV-1 Gag direct particle release through pathways linked by Tsg101. Traffic (Copenhagen, Denmark) 6 (10), 880–894.

Mitnaul, L.J., Castrucci, M.R., Murti, K.G., Kawaoka, Y., 1996. The cytoplasmic tail of influenza A virus neuraminidase (NA) affects NA incorporation into virions, virion morphology, and virulence in mice but is not essential for virus replication. J. Virol. 70 (2), 873–879.

Morita, E., Sundquist, W.I., 2004. Retrovirus budding. Annu. Rev. Cell Dev. Biol. 20, 395–425.

Mosley, V.M., Wyckoff, W.G.R., 1946. Electron micrography of the virus of influenza. Nature 157 (263).

Noton, S.L., Medcalf, E., Fisher, D., Mullin, A.E., Elton, D., Digard, P., 2007. Identification of the domains of the influenza A virus M1 matrix protein required for NP binding, oligomerization and incorporation into virions. J. Gen. Vir. 88 (Pt 8), 2280–2290.

Pilecka, I., Banach-Orlowska, M., Miaczynska, M., 2007. Nuclear functions of endocytic proteins. Eur J. Cell Biol. 86 (9), 533–547.

Pineda-Molina, E., Belrhali, H., Piefer, A.J., Akula, I., Bates, P., Weissenhorn, W., 2006. The crystal structure of the C-terminal domain of Vps28 reveals a conserved surface required for Vps20 recruitment. Traffic (Copenhagen, Denmark) 7 (8), 1007–1016.

Raymond, C.K., Howald-Stevenson, I., Vater, C.A., Stevens, T.H., 1992. Morphological classification of the yeast vacuolar protein sorting mutants: evidence for a prevacuolar compartment in class E vps mutants. Mol. Biol. Cell 3 (12), 1389–1402.

Reynwar, B.J., Illya, G., Harmandaris, V.A., Muller, M.M., Kremer, K., Deserno, M., 2007. Aggregation and vesiculation of membrane proteins by curvature-mediated interactions. Nature 447 (7143), 461–464.

Roberts, P.C., Compans, R.W., 1998. Host cell dependence of viral morphology. Proc. Natl. Acad. Sci. U. S. A. 95 (10), 5746–5751.

Roberts, P.C., Lamb, R.A., Compans, R.W., 1998. The M1 and M2 proteins of influenza A virus are important determinants in filamentous particle formation. Virology 240 (1), 127–137.

Rothman, J.H., Stevens, T.H., 1986. Protein sorting in yeast: mutants defective in vacuole biogenesis mislocalize vacuolar proteins into the late secretory pathway. Cell 47 (6), 1041–1051.

Rusten, T.E., Simonsen, A., 2008. ESCRT functions in autophagy and associated disease. Cell Cycle 7 (9), 1166–1172.

Sevrioukov, E.A., Moghrabi, N., Kuhn, M., Kramer, H., 2005. A mutation in dVps28 reveals a link between a subunit of the endosomal sorting complex required for transport-I complex and the actin cytoskeleton in Drosophila. Mol. Biol. Cell 16 (5), 2301–2312.

Silvestri, L.S., Ruthel, G., Kallstrom, G., Warfield, K.L., Swenson, D.L., Nelle, T., Iversen, P.L., Bavari, S., Aman, M.J., 2007. Involvement of vacuolar protein sorting pathway in Ebola virus release independent of TSG101 interaction. J. Infect. Dis. 196 (Suppl 2), S264–S270.

Simpson-Holley, M., Ellis, D., Fisher, D., Elton, D., McCauley, J., Digard, P., 2002. A functional link between the actin cytoskeleton and lipid rafts during budding of filamentous influenza virions. Virology 301 (2), 212–225.

Smirnov Yu, A., Kuznetsova, M.A., Kaverin, N.V., 1991. The genetic aspects of influenza virus filamentous particle formation. Arch. Virol. 118 (3–4), 279–284.

Stuffers, S., Brech, A., Stenmark, H., 2008. ESCRT proteins in physiology and disease. Exp. Cell Res. 315 (9), 1619–1626.

Taylor, G.M., Hanson, P.I., Kielian, M., 2007. Ubiquitin depletion and dominant-negative VPS4 inhibit rhabdovirus budding without affecting alphavirus budding. J. Virol. 81 (24), 13631–13639.

Teo, H., Gill, D.J., Sun, J., Perisic, O., Veprintsev, D.B., Vallis, Y., Emr, S.D., Williams, R.L., 2006. ESCRT-I core and ESCRT-II GLUE domain structures reveal role for GLUE in linking to ESCRT-I and membranes. Cell 125 (1), 99–111.

Utley, T.J., Ducharme, N.A., Varthakavi, V., Shepherd, B.E., Santangelo, P.J., Lindquist, M. E., Goldenring, J.R., Crowe Jr, J.E., 2008. Respiratory syncytial virus uses a Vps4-independent budding mechanism controlled by Rab11-FIP2. Proc. Natl. Acad. Sci. U. S. A. 105 (29), 10209–10214.

von Schwedler, U.K., Stuchell, M., Muller, B., Ward, D.M., Chung, H.Y., Morita, E., Wang, H.E., Davis, T., He, G.P., Cimbora, D.M., Scott, A., Krausslich, H.G., Kaplan, J.,

Morham, S.G., Sundquist, W.I., 2003. The protein network of HIV budding. Cell 114 (6), 701–713.
Wang, M.Q., Kim, W., Gao, G., Torrey, T.A., Morse 3rd, H.C., De Camilli, P., Goff, S.P., 2003. Endophilins interact with Moloney murine leukemia virus Gag and modulate virion production. J. Biol. 3 (1), 4.
Welsch, S., Habermann, A., Jager, S., Muller, B., Krijnse-Locker, J., Krausslich, H.G., 2006. Ultrastructural analysis of ESCRT proteins suggests a role for endosome-associated tubular-vesicular membranes in ESCRT function. Traffic (Copenhagen, Denmark) 7 (11), 1551–1566.
Williams, R.L., Urbe, S., 2007. The emerging shape of the ESCRT machinery. Nat. Rev., Mol. Cell. Biol. 8 (5), 355–368.
Yuan, B., Campbell, S., Bacharach, E., Rein, A., Goff, S.P., 2000. Infectivity of Moloney murine leukemia virus defective in late assembly events is restored by late assembly domains of other retroviruses. J. Virol. 74 (16), 7250–7260.